NASA TECHNICAL NOTE

NASA TN D-3070

NASA TN D-3070

OPERATIONAL AND PERFORMANCE CHARACTERISTICS OF THE X-15 SPHERICAL, HYPERSONIC FLOW-DIRECTION SENSOR

by Chester H. Wolowicz and Terrence D. Gossett

Flight Research Center
Edwards, Calif.

NATIONAL AERONAUTICS AND SPACE ADMINISTRATION - WASHINGTON, D. C. - NOVEMBER 1965

NASA TN D-3070

OPERATIONAL AND PERFORMANCE CHARACTERISTICS OF THE X-15 SPHERICAL, HYPERSONIC FLOW-DIRECTION SENSOR

By Chester H. Wolowicz and Terrence D. Gossett

Flight Research Center
Edwards, Calif.

NATIONAL AERONAUTICS AND SPACE ADMINISTRATION

For sale by the Clearinghouse for Federal Scientific and Technical Information
Springfield, Virginia 22151 – Price $1.00

ABSTRACT

The basic design concepts, operational experiences (malfunctions, system characteristics, and system improvements), and flight-data measurements of the sensor are discussed and analyzed. The accuracy of the sensor in measuring angle of attack and angle of sideslip is assessed on the basis of an analysis of flight data and comparisons of these data with X-15 flight data determined from vane-type nose-boom installations and X-15 wind-tunnel data. Some practical limitations in the use of the sensor for extreme altitude applications are also considered.

OPERATIONAL AND PERFORMANCE CHARACTERISTICS OF THE X-15 SPHERICAL, HYPERSONIC FLOW-DIRECTION SENSOR

By Chester H. Wolowicz and Terrence D. Gossett
Flight Research Center

SUMMARY

The basic design concepts, flight-data measurements, and operational experiences, including malfunctions, system characteristics, and system improvements, of the X-15 spherical, hypersonic flow-direction sensor are discussed and analyzed. The accuracy of the sensor in measuring angle of attack and angle of sideslip is assessed on the basis of an analysis of flight data and comparisons of these data with X-15 flight data obtained from vane-type nose-boom installations and X-15 wind-tunnel data. Some practical limitations in the use of the sensor for extreme altitude applications are also considered.

Early developmental and utilization problems were alleviated and the reliability of the sensor was enhanced by improved inspection techniques to minimize hydraulic contamination, replacement of vibration-sensitive components by insensitive components, and replacement of quick-disconnect features on plumbing with stainless-steel fittings, which comply with military specifications. Improved dynamic characteristics were realized by replacing the synchro receiver with a passive rotor driven by a servorecorder. A potentially dangerous 12-cycle-oscillation limit-cycle characteristic was alleviated by exchanging the electronic gain for a mechanical gain.

Although a direct comparison with other sensors was not possible because of operational limitations, flight results showed a good consistency in sensor data at discrete Mach numbers at dynamic pressures above 20 lb/sq ft. The spherical-sensor data correlated well with corresponding vane-boom data up to a Mach number of about 3. A comparison with faired wind-tunnel data showed good correlation in the slope of normal-force coefficient versus angle of attack up through Mach 5.8 and in the absolute magnitudes of these quantities up to Mach 3.

At low dynamic pressures on the order of 40 lb/sq ft and less and at high angles of attack of approximately 26° and higher, the collar of the spherical-sensor housing may have caused flow interference, which resulted in a flareup in angle-of-attack indications. Degradation in system accuracy became appreciable at dynamic pressures below 10 lb/sq ft. At dynamic pressures of the order of 3 lb/sq ft or less, the pitch and yaw reaction jets of the X-15 ballistic control system affected the flow field over the sphere of the sensor, causing erroneous indications.

INTRODUCTION

From the inception of the X-15 program, it was apparent that a new sensor would have to be developed for measuring angles of attack and sideslip in order to overcome the operational limitations of the NASA vane-type, nose-boom-mounted sensors (ref. 1) in the hypersonic region of flight and at high altitudes. The operational limits of the nose-boom installation are governed by the vulnerability of the boom to high temperatures at high dynamic pressures during hypersonic flight in the atmosphere, and by the increase in vane position error due to a decrease in accuracy of the nose-boom air-flow-direction measurements above a Mach number of 3.0 and also at low dynamic pressures. The spherical, hypersonic flow-direction sensor, shown in comparison with the vane-type sensor in figures 1(a) and 1(b), was developed to overcome these operational limitations and to advance the state of the art in measuring angle of attack and angle of sideslip in the hypersonic regions up to a Mach number of approximately 7.

The primary function of the spherical sensor--commonly referred to as the "ball-nose-sensor" because of its location and shape--is to measure angle of attack and angle of sideslip; however, in certain regions of flight, it was found possible to use the sensor to measure total pressure, from which dynamic pressure could be determined (ref. 2). The importance of angle of attack and angle of sideslip in performing particular flight maneuvers or missions makes the precision of the measurement of these two quantities a matter of prime concern, both for data measurements and for display of the quantities to the pilot.

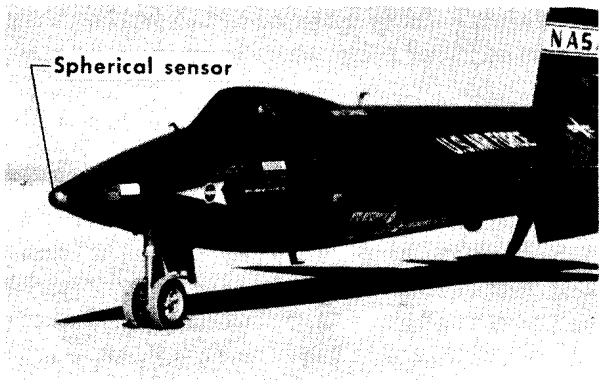

E-13659

(a) Spherical sensor.

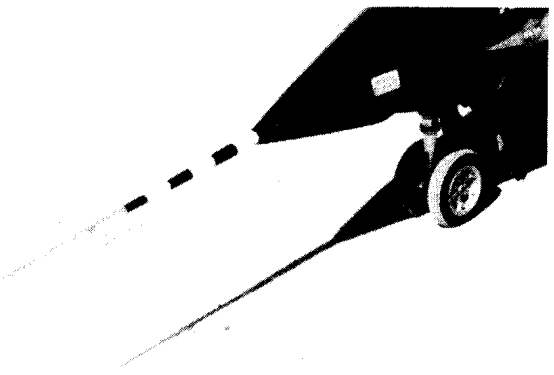

E-5251

(b) Boom-mounted vane-type sensor.

Figure 1.– Photographs of spherical and vane-type flow-direction sensors installed on the X-15 airplane.

Although adequate preflight laboratory and ground checkout tests of the sensor were performed, combined environmental tests were limited. Moreover, the pace of the X-15 flight program made it advisable to install the spherical sensor on the airplane at a time when only limited low-speed wind-tunnel calibration data from the sensor were available (ref. 3). Thus, the performance and operational characteristics of the sensor had to be determined under actual operational conditions and from flight data.

This paper documents the operational and performance characteristics of the spherical angle-of-attack and

angle-of-sideslip sensor system as an integral part of the X-15 airplane. Factors influencing the accuracy of the integrated system were determined by using comparative flight and wind-tunnel data.

SYMBOLS

a_n	normal acceleration, g units
a_y	transverse acceleration, g units
C_N	normal-force coefficient, $a_n\left(\frac{W}{qS}\right)$
C_Y	side-force coefficient, $a_y\left(\frac{W}{qS}\right)$
M	Mach number
q	dynamic pressure, lb/sq ft
S	wing area, sq ft
W	weight, lb
α	angle of attack, deg
β	angle of sideslip, deg
γ	flight-path angle, deg
θ	inertial pitch attitude, deg

THE AIRPLANE

The X-15 airplane (fig. 1), on which the spherical flow-direction sensor was installed, is a single-place, rocket-powered research airplane designed for high-speed and high-altitude research. The airplane has been flown to altitudes in excess of 350,000 feet, to speeds higher than Mach 6, and at angles of attack greater than 26°. The high-altitude capability of the vehicle necessitated the incorporation of reaction jets to supplement the aerodynamic controls in order to provide adequate control and damping throughout the flight envelope.

The reaction control system, frequently referred to as the ballistic control system, is a hydrogen-peroxide monopropellant jet (or rocket) system with pitch and yaw jets located just to the rear of the spherical flow-direction sensor (fig. 2) and roll jets on the outboard portions of the wing. The figure shows only the yaw reaction jets on the left side of the fuselage and the pitch

reaction jets on the lower portion of the fuselage. Additional jets are located similarly on the right side and the top of the fuselage.

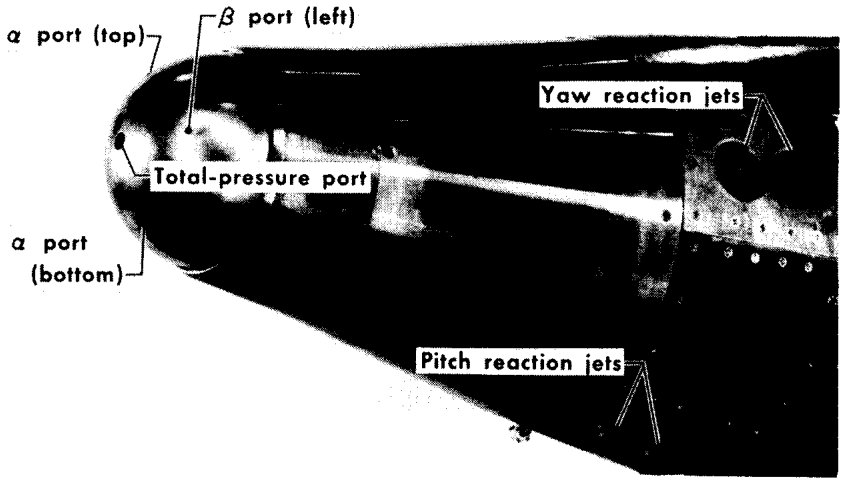

Figure 2.– Spherical flow-direction sensor and ballistic-control-system pitch and yaw reaction-control nozzles.

DESCRIPTION OF THE FLOW-DIRECTION SENSOR

The hypersonic, spherical flow-direction sensor (see closeup view, fig. 2) is a null-seeking, hydraulically operated, electronically controlled servomechanism. Pressure measurements, which are the sensor's sole inputs, consist of measuring the differential pressure of each of two pairs of static-pressure ports located 42° from the reference line in the vertical and horizontal planes (figs. 2 and 3) to determine flow direction in terms of angle of attack and angle of sideslip, and measuring total pressure along the reference line to determine dynamic pressure.

The sensor, designed by the Nortronics Division of Northrop Corp. for the National Aeronautics and Space Administration, has a 6.5-inch-diameter sphere made of Inconel X to resist high temperatures encountered in X-15 flights. The overall length of the sensor is 16.7 inches and, as shown in figure 3, the rear portion contains the mechanical and electrical components. These components, along with the sphere, are cooled by vaporized liquid nitrogen as needed. When mounted on the X-15 airplane, the sensor operates from the vehicle's electrical, hydraulic, and coolant inputs. Electrically, the sensor operates on 28-volt dc and 115-volt, 400 cycle ac current; hydraulically, it uses Oronite 8515 fluid at 3000 lb/sq in. Power consumption is 75 watts and 30 watts on the 28-volt and 115-volt circuits, respectively.

The sensor operates on the principle that when two static ports are located on a sphere, a null reading in the differential pressure of the two

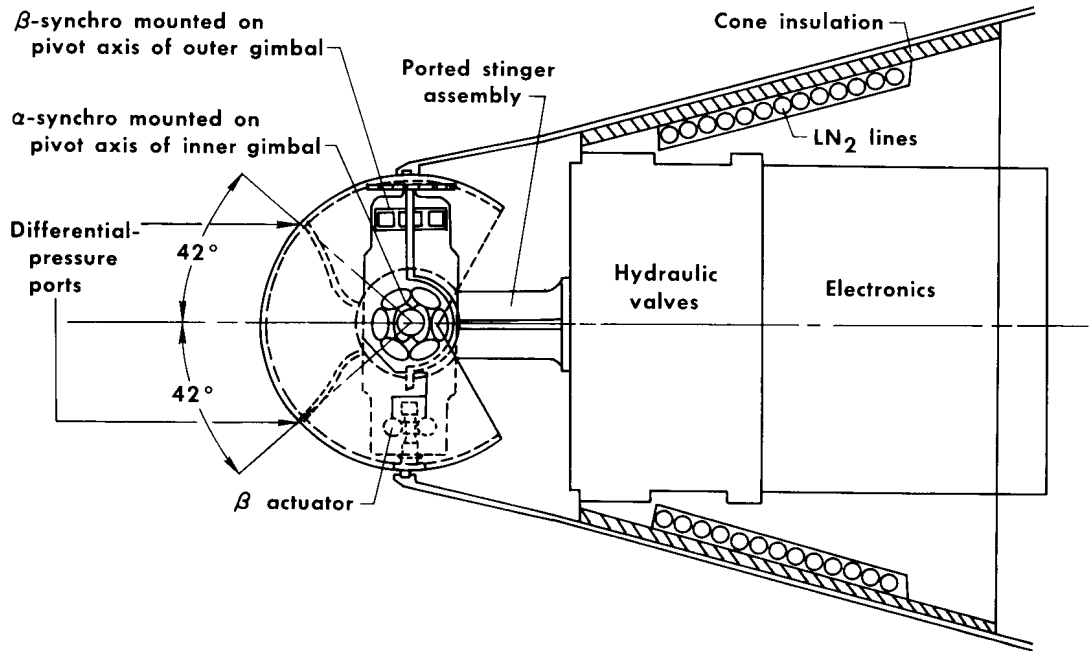

Figure 3.– Schematic drawing of NASA spherical flow-direction sensor.

ports will result if the bisector of the included great-circle angle of the ports is collinear with the resultant velocity vector immediately in front of the sphere. The inclination of the velocity vector relative to a reference in the plane of the great circle is given by the angle formed by the bisector and the reference.

On the sensor itself, each pair of null-seeking ports is connected to a differential-pressure transducer (fig. 4). The unbalanced pressure in the transducer activates an electrical signal, which causes a hydraulic actuator to position the sphere to zero differential pressure. Since the sensor was designed to have an operational accuracy of ±0.25° within the dynamic-pressure range from 15 lb/sq ft to 2500 lb/sq ft, a q-compensator transducer (see figure) provides proper gain compensation to the α and β circuits for the large change in differential pressures sensed by the α and β transducers. Since an electromechanical technique is used in the gain-compensation subsystem, the subsystem has q-rate limitations; however, the gain-compensation subsystem has been redesigned to meet the constraint of q-rate requirements during the reentry portion of high-altitude trajectories.

Positioning of the sphere is dependent on a two-gimbal pivot system. The sphere constitutes the outer gimbal which is pivoted to the inner gimbal (fig. 3), whose pivotal axis is fixed normal to the plane of symmetry of the airplane. As the sensing sphere seeks null readings in each of its two pairs of static-pressure ports, the gimbals rotate about their respective axes. The inner gimbal, rotating about its fixed axis, sweeps an angle α in the plane of symmetry; the magnitude of the angle is picked off by an α-synchro (7-minute accuracy) located on the fixed pivotal axis. The outer gimbal, whose pivotal

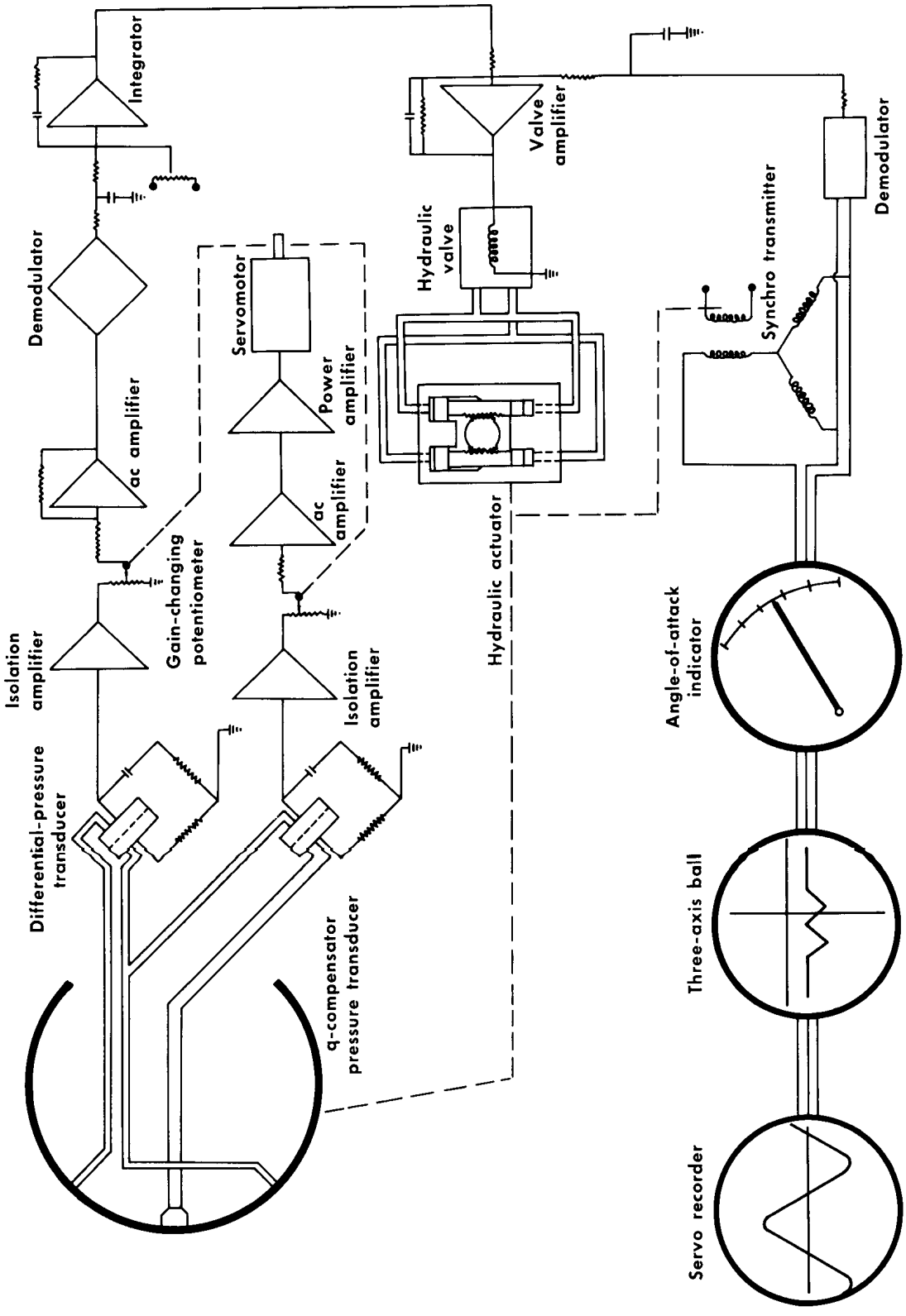

Figure 4.– Functional diagram of the angle-of-attack portion of the spherical flow-direction-sensor system. (Angle-of-sideslip portion of system is similar.)

axis is mounted on the inner gimbal and remains in the plane of symmetry at all times, sweeps an angle β in a plane which is perpendicular to the plane of symmetry. This plane is the transverse plane of the stability-axis system of the aircraft. The β angle is picked off by the β control transmitter synchro on the outer-gimbal pivotal axis (fig. 3). Because of the gimbal arrangement, the α and β angles picked off by the synchros are stability-axis-system angles of the airplane. The α and β outputs of the sensor are transmitted by the synchros to on-board recorders and to the pilot's display panel, as indicated in figure 4. On the three-axis-ball presentation, a cross-bar display of α and β is included for nulling purposes in specific flight regimes.

DEVELOPMENT TESTING

During the early stages of the sensor development, many laboratory tests were made by Nortronics to evaluate system performance. The tests included standard atmospheric operation, voltage and frequency variation, dynamic response (sinusoidal and linear inputs), low-temperature operation, high-temperature operation, acceleration, vibration, and endurance. Details of these tests are recorded in reference 3.

In addition to the Nortronics tests, thermal shock tests were performed at the NASA Flight Research Center to demonstrate the ability of the flow-direction sensor to withstand the effects of thermal shock. The jet exhaust of an F-100 airplane equipped with an afterburner was used as the source of heat. The sensor, completely instrumented with thermocouples, was positioned 14 inches aft of the F-100C variable-geometry tailpipe at an angle of attack of 14° relative to the exhaust stream. The thermal tests were designed to build up the sensor temperature on successive runs to the qualifying 1300° F. Each run was time-limited, and the test results were examined carefully in order to program the time of operation for the following run. In a typical run, the engine was brought to 100-percent power (in approximately 50 seconds), the afterburner was applied for an exact time interval (5 seconds on first run, 7 seconds on second run), the engine was run for 2 minutes without afterburner, and then shut down. During the runs, a sinusoidal signal of ±10° in pitch and yaw at 0.5 cycle per second was commanded to the sensor servos to operate the sensor. Cold tests, to -100° F, were also made at the Flight Research Center.

No wind-tunnel tests, with the exception of low-velocity tests over a dynamic-pressure range from 0.5 lb/sq ft to 45 lb/sq ft in the Northrop 7- by 10-foot tunnel, were conducted to calibrate the ball-nose sensor throughout the Mach number range of the X-15 airplane. Upwash corrections resulting from the Northrop tunnel tests are included in reference 4.

FLIGHT-TEST CONDITIONS

Flight data were obtained from the flight records of the X-15 research missions, encompassing a flight environment in which dynamic pressures ranged

from less than 1 lb/sq ft to 2027 lb/sq ft, Mach number and altitude reached 6.06 and 354,200 feet, respectively, and flow-direction angles extended to approximately 26°. In performing the required missions, altitude trajectories, push down—pull up maneuvers, and essentially constant-altitude acceleration-deceleration runs at high dynamic pressures and temperatures were flown. Data presented at each of the representative Mach numbers used in this paper were selected at nearly steady-state conditions.

RESULTS AND DISCUSSION

Operational Problems

During the X-15 flight program, the developmental problems that occurred with the sensor were related primarily to static alinement, component failures, recorder feedback effects, and limit cycle (4 cps and 12 cps).

Alinement.— Static alinement of the ball-nose sensor with the X-15 reference axis was accomplished initially by means of transits placed at two locations: (1) abeam of the vehicle for longitudinal alinement and (2) in front of the X-15 for lateral alinement. Alinement accomplished by this method prior to each X-15 flight was tedious, time-consuming, and had inherent angular-resolution difficulties. Hence, an alternate technique was devised consisting of a quick-mounted jig attached to the movable sensor sphere. The jig includes a telescope (with a vertical crosshair) that can be mounted in the aircraft symmetry plane, thus enabling establishment of 0° angle of sideslip through alinement of the crosshair with reference points on the X-15 upper fuselage. Zero angle of attack is ascertained by correlating clinometer measurements of the aircraft reference pitch-angle plane (canopy rail) to a corresponding angle-of-attack plane from the sensor (represented by a flat surface on the alinement jig). Estimated accuracy of static alinement for both α and β with the NASA technique is 7 minutes of arc.

Component failures.— Some components of the spherical flow-direction-sensor system have been more susceptible to failure than others. These components are the hydraulic servovalves, differential-pressure transducers, and silicone rubber pneumatic lines within the sensor pneumatic system.

The hydraulic servovalves are very sensitive to fluid contamination; however, special precautions to insure cleanliness have alleviated this problem. The primary reason for the four valve failures was O-ring abrasion from normal usage, with the result that O-ring particles contaminated the ball-nose system. Three of the four valve failures were discovered in the laboratory during normal preventive-maintenance checks on the sensor; replacement of each faulty valve remedied the problem. The fourth hydraulic-valve failure was manifested in flight by intermittent, low-amplitude (±0.2° to ±0.3°), four-cycle oscillations. Replacement of the valve eliminated the oscillation.

The differential-pressure transducers are delicate instruments which slowly succumb to the rigors of flight vibration, thermal cycling, and diaphragm flexing. Possible corrective action is limited by transducer state of

the art. In the course of standard laboratory preventive-maintenance testing, four transducers have been replaced, each for degraded signal output. The degradation in each transducer was due to a nonlinearity between input pressure to the transducer and output voltage. The operational effect of a small nonlinearity in either the gain-compensation transducer or α and β transducers would be either slightly higher or lower system sensitivity, depending upon the relative polarity of the nonlinearity error. In each of the four transducer problems discovered through laboratory testing, deficiencies were not perceivable in flight.

The silicone rubber pneumatic-line problems consisted of line and connection failures. The line failures were eliminated by the simple expedient of closer visual inspection of the tubing within the sensor. Only two tubing failures have occurred, and both were detected through preflight testing of the sensor. However, the sensor aft pneumatic-disconnect fitting within the pneumatic system was the source of two partial pneumatic failures. These partial failures were characterized by a cycling pressure drop of approximately 200 lb/sq ft in the total-pressure line when the total pressures exceeded 1700 lb/sq ft. This action, revealed through routine sensor checkout before each of two X-15 flights, was the result of overload on the O-ring in the quick-disconnect fitting. Inasmuch as the flights involved total pressures less than 1700 lb/sq ft, the flights were not adversely affected. The quick-disconnect fittings have been replaced by stainless-steel fittings that comply with military specifications, thus minimizing leak possibilities at this junction.

To improve the overall operational efficiency of the components, the following changes in the system were necessary:

(1) Quick-disconnect features of hydraulic, liquid-nitrogen, and pneumatic lines in the rear of the sensor were replaced by stainless-steel fittings because of leak and safety considerations.

(2) Hydraulic-actuator stinger assemblies were changed from a two-piece to a one-piece construction to eliminate hydraulic seepages.

(3) Original liquid-nitrogen valves were replaced by valves insensitive to vibration.

The ball nose was originally installed on the X-15 in December 1960 and has been operational, from launch to landing, on all but one flight of the airplane.

Recorder feedback effects.– Initially, the synchro transmitters of the sensor were coupled with synchro receivers for the purpose of recording data, as were the vane-boom synchro transmitters previously used. However, within the spherical sensor, a portion of the signal from the synchro transmitters is used for degenerative feedback, thus lowering the gain of the α and β inner-positional servo loops. This feedback-utilization technique is basically stable but causes instabilities in the sensor servomechanism when used with a recorder of the synchro-receiver type. The problem arises from the excited rotor contained within the synchro receiver, which acts as a transmitter when

(a) Vane boom and synchro recorder.

(b) Spherical sensor and synchro recorder.

(c) Spherical sensor and servo recorder.

Figure 5.– Relative time histories of sensor systems equipped with synchro recorder and servo recorder.

used as described. The problem was solved by replacing the synchro recorder with a servo recorder which incorporates a passive rotor. Figures 5(a) to 5(c) show comparative time histories of the vane-boom and spherical sensors equipped with synchro receiver recorders and the spherical sensor equipped with a recorder which has a passive rotor driven to null (servo recorder). This figure indicates that the spherical sensor oscillates when it is used with a synchro receiver recorder and that the oscillation is minimized when a servo recorder is used.

Limit-cycle characteristics.– In addition to the oscillations previously discussed, 12-cycle oscillations were experienced in the output of the spherical sensor at low dynamic pressures (35 lb/sq ft to 150 lb/sq ft) and rates of change of dynamic pressure exceeding 5 lb/sq ft per second. These oscillations posed a problem, inasmuch as it was desired that sensor signals for angle of attack be used by the adaptive flight control system in one of the X-15 airplanes during the reentry portion of flight. The 12-cycle oscillations were transmitted to the aircraft controls through the autopilot, which resulted in a hazardous condition, since the airframe resonant frequency is also 12 cps. The cause of the oscillation problem within the ball nose was a rate-limited servomechanism (the q-gain compensation system). The purpose of the compensation is to maintain constant servo-loop gains in the α and β circuits and, thus, dynamic-pressure independency. However, when dynamic pressure is low, which necessitates large gain compensation, and increases at a rapid rate (i.e., reentry), actual gain compensation markedly lags and is greater than required compensation. This lag is inherent in the servosystem; the wiper of the feedback potentiometer cannot attain the required position because the servomotor is unable to keep up with signal error corresponding to dynamic pressure. This period of excessive gain may exceed the sensor closed-loop 6-decibel-gain margin for some transient time, thus causing oscillation at the sensor's natural frequency of 12 cps until the potentiometer wiper advances sufficiently. The problem was solved by decreasing the electronic gain and increasing the mechanical gain of the gain-compensation loop. The loop gain is kept constant and, consequently, the wiper of the feedback potentiometer does not lag appreciably.

Four-cycle oscillations were also experienced on random occasions (see fig. 6). The oscillations were believed to be due, in part, to the X-15 3000-lb/sq in. hydraulic system which has pressure pulsations of ±400 lb/sq in. when hydraulic controls are being actuated. Another source of the oscillations is believed to be the hydraulic servovalves within the spherical sensor, inasmuch as the oscillation problem was corrected in one instance, as related

earlier, by replacing the valve. Because these oscillations are infrequent and are of small amplitude, they are not of major concern.

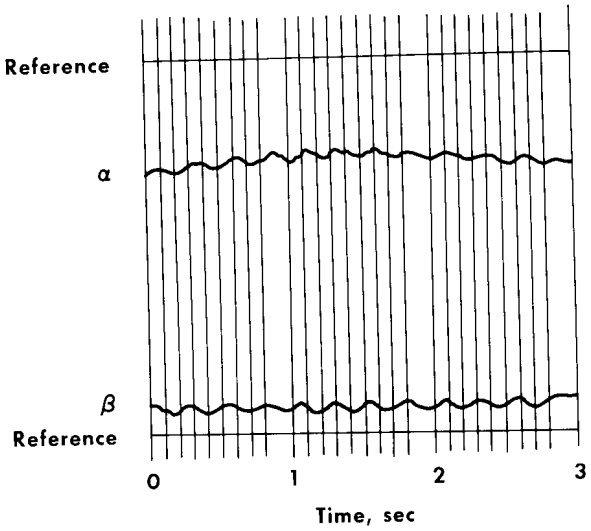

Figure 6.– Time history of four-cycle oscillations that appeared on records on random occasions.

Flight Performance of the Sensor

Operational limitations precluded the simultaneous installation of accurate vane-type, boom-mounted α and β sensors as prime, on-board references for the spherical flow-direction sensor. Thus, it was necessary to resort to indirect means, discussed in the following sections, to evaluate the flight performance of the sensor.

Angle-of-attack measurements at $q > 20$ lb/sq ft.– To check the consistency of angle-of-attack values obtained from the spherical sensor, angles of attack recorded from many flights were plotted against flight-determined values of airplane normal-force coefficient for dynamic pressures above 20 lb/sq ft at discrete Mach numbers. These results, shown in figure 7, indicated that the data were generally within ±0.5° with respect to a faired curve at each Mach number. The data at M = 0.8 were corrected for upwash effects, as determined from wind-tunnel tests (ref. 4). These upwash effects were appreciable at subsonic speeds, producing indicated angles of attack or sideslip approximately

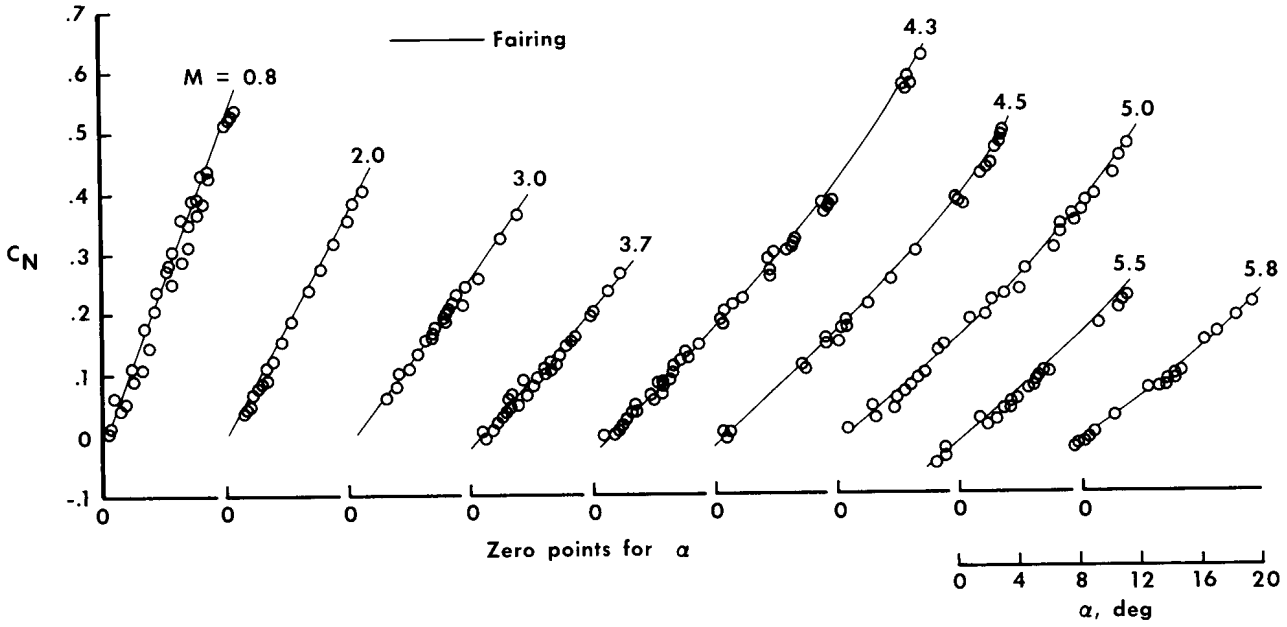

Figure 7.– Variation of normal-force coefficient with angle of attack measured in flight by spherical sensor. Speed brakes closed; $q > 20$ lb/sq ft.

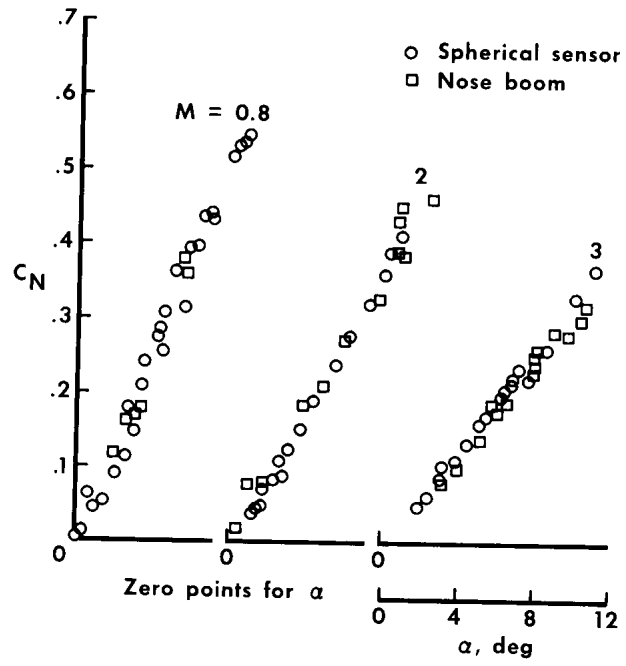

Figure 8.– Comparison of variation of normal-force coefficient with angle of attack measured in flight by spherical sensor and with nose-boom α-vane. Speed brakes closed; q > 20 lb/sq ft.

50 percent greater than true values; quantities of these parameters displayed in flight were similarly in error, which required extra pilot attention when flying in this speed range.

A comparison of the variation in flight-determined C_N with α determined by the spherical sensor and by the nose-boom α-vane at Mach numbers of 0.8, 2.0, and 3.0 is shown in figure 8. The figure shows good correlation of the data. Inasmuch as the synchro transmitter and receiver of the boom-mounted α-vane sensor have manufacturer's quoted accuracies of ±0.5° and are the least-accurate portion of the vane-boom system, it may be assumed, on the basis of the comparisons in figure 8, that the angle-of-attack portion of the spherical sensor also has this, or better, accuracy up to M = 3.0.

A comparison, in figure 9, of the faired flight data from the ball-nose

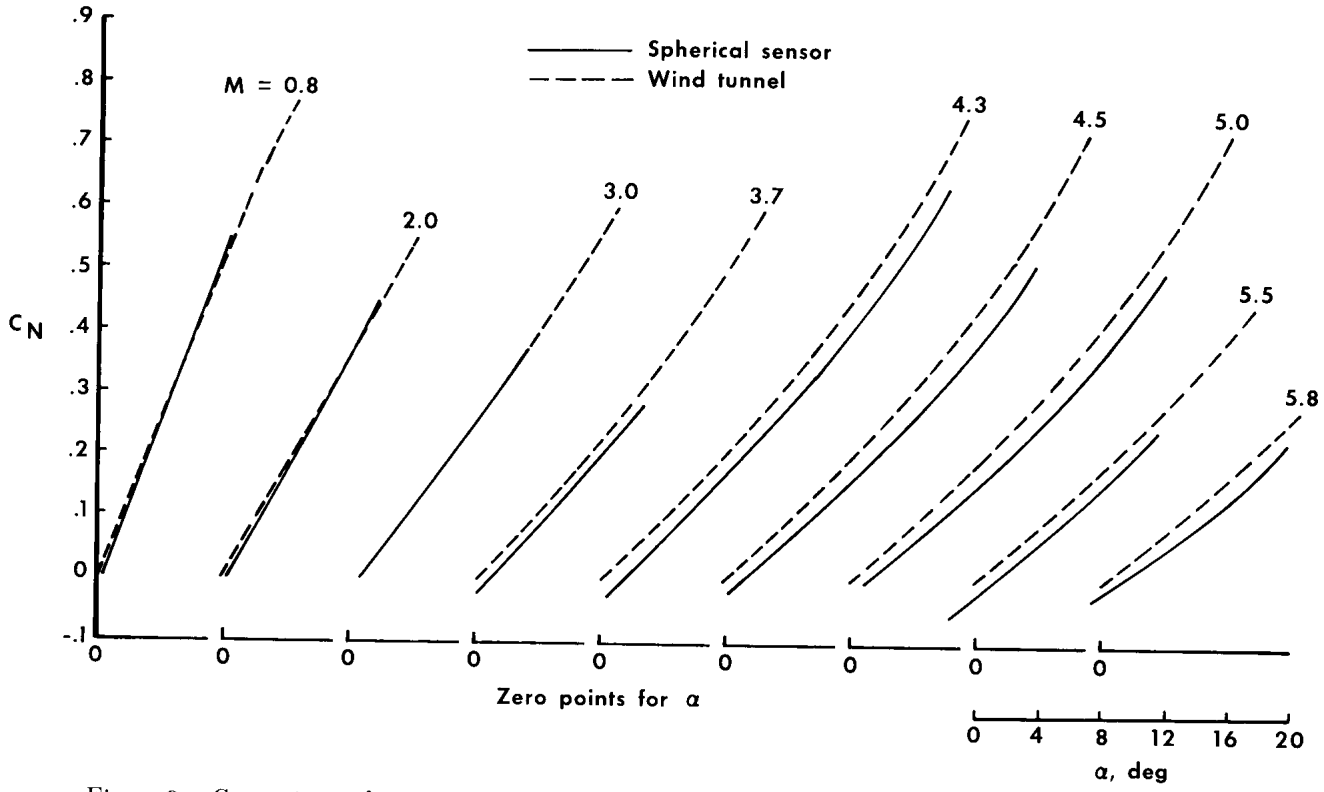

Figure 9.– Comparison of variation of normal-force coefficient with angle of attack of spherical-sensor flight data with wind-tunnel data. Speed brakes closed; q > 20 lb/sq ft.

sensor with faired wind-tunnel data obtained with X-15 models shows good correlation of the slopes of C_N versus α at all Mach numbers. For Mach numbers at and below M = 3.0, the absolute values of the data are in good agreement; however, at higher Mach numbers a discrepancy of about 1° to 1.5° exists between the flight and wind-tunnel angles of attack for given values of C_N. Although complete correlation is not expected, the fact that the data agreed well at and below M = 3.0 but showed a discrepancy at higher Mach numbers is difficult to explain. Some of the discrepancy may lie in the fact that wind-tunnel data were taken from faired measured data obtained in several facilities (ref. 5). In addition, the aircraft is not an absolutely rigid structure, and the flight data were obtained from various types of maneuvers.

All factors considered, the spherical sensor is believed to be inherently accurate to better than ±0.5° within the angle-of-attack range of the flight data shown in figure 9, that is, up to approximately 22° at dynamic pressures above 20 lb/sq ft.

During reentry from high altitude, the X-15 airplane, in addition to experiencing low dynamic pressures, occasionally undergoes high-angle-of-attack conditions of the order of 26° and higher. Records typified by the traces in figures 10 and 11 appear to indicate that the sensor system will sometimes provide erroneous angular indications when the angle of attack is higher than approximately 26° and dynamic pressure is less than approximately 40 lb/sq ft. Figure 10 shows that the indicated angle of attack flared from approximately 26° to 36° during reentry in the dynamic-pressure region of approximately 31 lb/sq ft to 60 lb/sq ft. This flaring is not in agreement with the magnitude of pitch-attitude changes shown, inasmuch as the flight-path angle (equal to $\theta - \alpha$ for a wings-level condition) changes slowly in this portion of the reentry. Since the reaction control system in pitch was active during the initial phase of this flareup as well as during the portion shown in figure 10, it may have been a strong factor in inducing the flareup. Figure 11 shows, however, that the same phenomenon

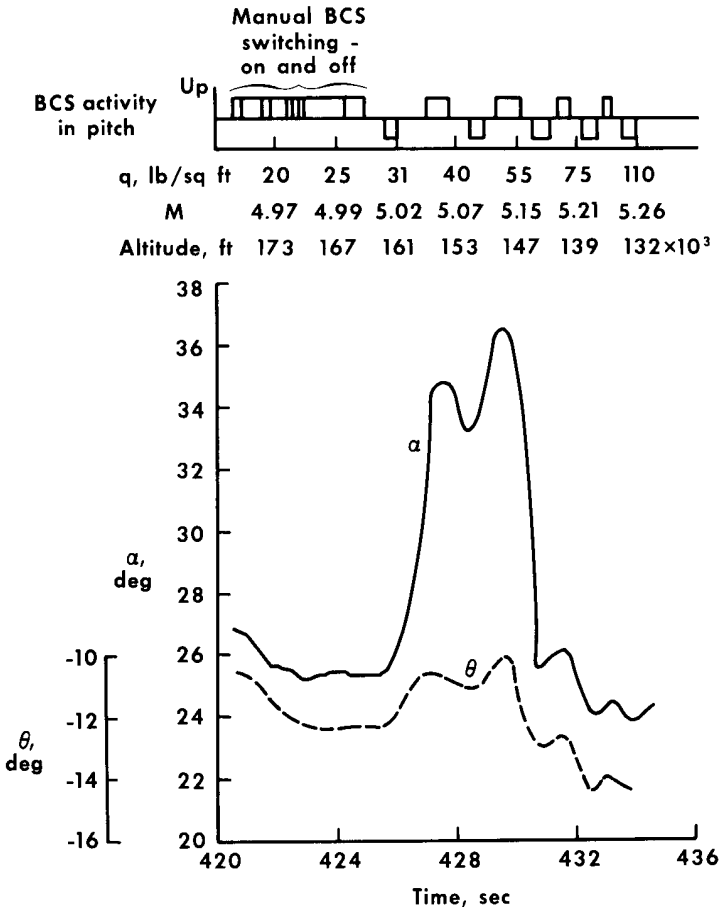

Figure 10.– Time history of flareup in angle-of-attack indications of spherical sensor during reentry. Ballistic control system (BCS) active in pitch only.

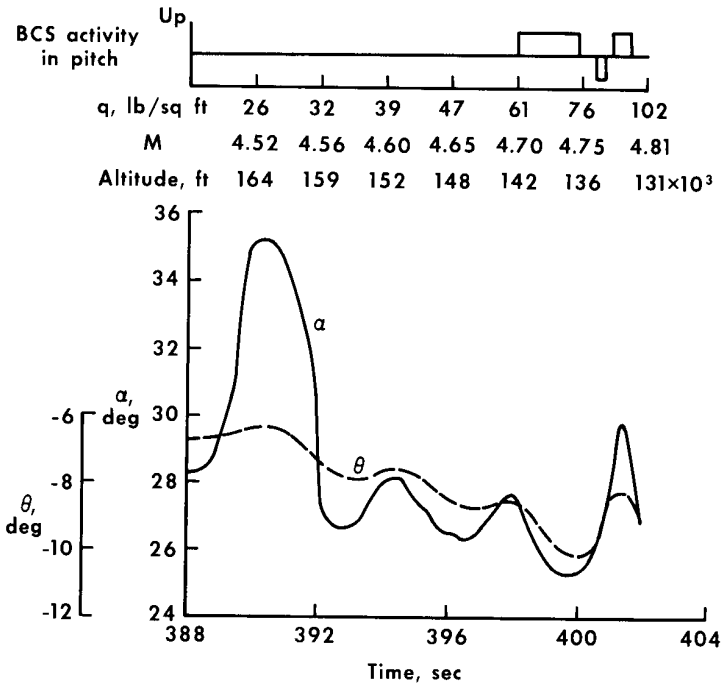

Figure 11.– Time history of flareup in angle-of-attack indications of spherical sensor during reentry. Ballistic control system (BCS) inactive during flareup.

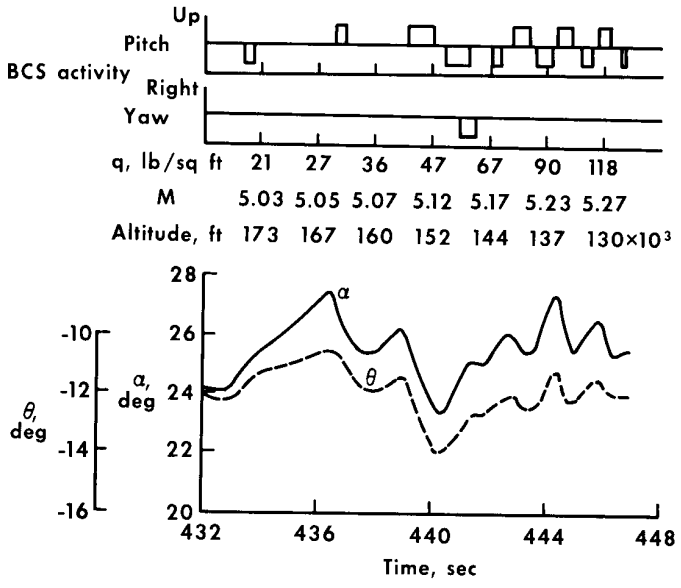

Figure 12.– Time history of angle-of-attack indications of spherical sensor during reentry showing incipient tendency toward flareup at approximately 433.5 seconds at $\alpha \approx 24^{o}$.

occurred in the absence of the reaction-control activity under similar situations when the preflare angle of attack was approximately 28°. A possible incipient tendency toward flareup is shown in figure 12 at approximately 433.5 seconds at $\alpha = 24°$; however, reaction-control activity in pitch to increase negative pitch attitude at 436.5 seconds appears to have countered the tendency. Although the specific causes of this phenomenon are not positively identified, it appears that the lip of the collar of the sphere housing may be causing flow interference that affects the angle-of-attack port nearest the collar and, thus, results in a flareup in the angle-of-attack indications. This tendency may be compounded by the dynamic-pressure rate limitations of the sensor's gain-compensation system (potentiometer wiper lag).

Angle-of-attack measurements at $q < 20$ lb/sq ft.– Inasmuch as the nulling action of the spherical sensor depends upon the differential pressure across the static ports and the gains of the servo system are dependent upon the dynamic pressure, it was anticipated that the accuracy of the spherical sensor would deteriorate at low dynamic pressures. Measured and analytical angle-of-attack errors are compared in figure 13 for dynamic pressures between 3 lb/sq ft and 10 lb/sq ft. The measured

angles of attack were obtained from the relationship $\alpha = \theta - \gamma$ and, for the data selected, were for $\gamma = 0°$. In these calculations, pitch-attitude measurements were obtained from the inertial-system output, and the flight-path measurements were obtained from radar data. It should be noted that the accuracy of the flight-path-angle determination is fairly limited.

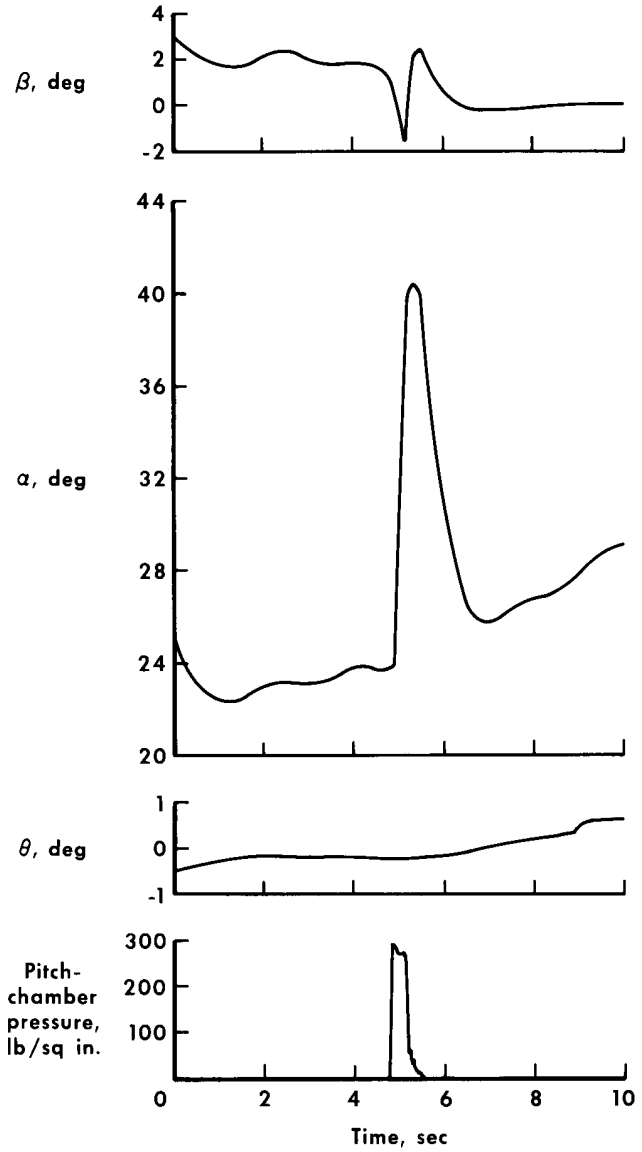

Figure 14.– Typical time history of flow interference due to ballistic-control inputs at very low dynamic pressure. M = 4.64 to 4.52; q = 1 to 2.5 lb/sq ft.

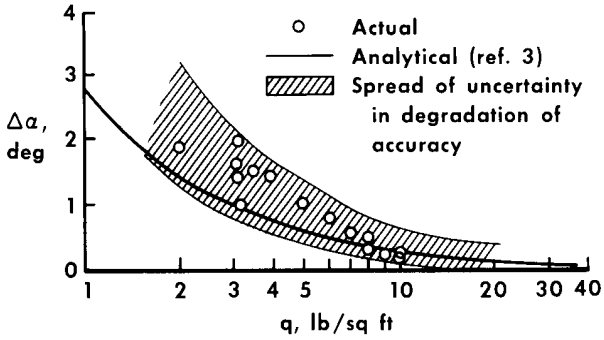

Figure 13.– Accuracy of spherical flow-direction sensor at low dynamic pressures. $\Delta\alpha = \alpha_{sensor} - (\theta_{inertial} - \gamma_{radar})$.

The accuracy of the spherical sensor appears to be good down to a dynamic pressure of 10 lb/sq ft. The degradation in accuracy is appreciable at much lower dynamic pressures, as indicated in figure 13. However, for the X-15 airplane, the sensor performance is considered to be satisfactory at the low dynamic pressures shown. Errors at these low pressures are less critical than those in regions of high dynamic pressure, inasmuch as the pilots rely on the pitch attitude in this region during the ballistic-trajectory phase of X-15 altitude flights.

During the ballistic phase of the altitude flights in the rarefied atmosphere, airplane attitudes are controlled by the ballistic control system (BCS) which utilizes pitch and yaw reaction jets positioned just behind the spherical sensor (fig. 2) and roll reaction jets near the wing tips. Activation of the reaction jet for pitch control has a significant effect on the flow field forward of the jet nozzle at very low dynamic pressures. As shown in figure 14, which encompasses a dynamic-pressure range from 1 lb/sq ft to 2.5 lb/sq ft, activation of the BCS for pitch

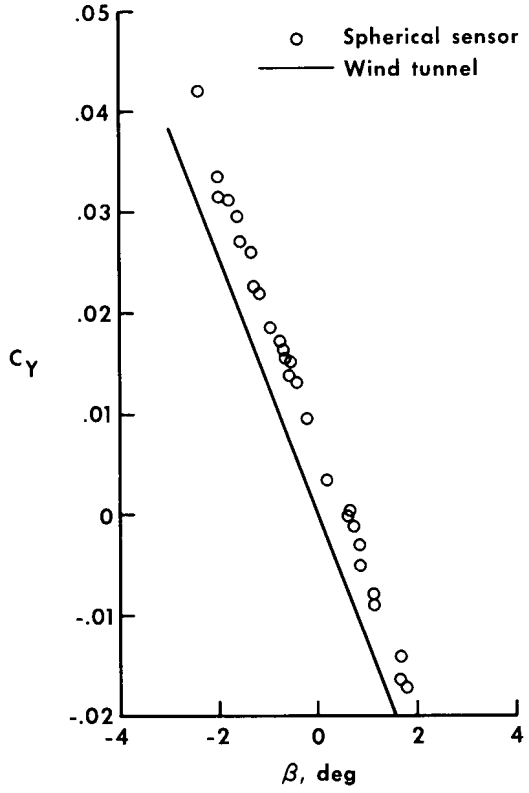

Figure 15.– Comparison of wind-tunnel and flight-determined variation of side-force coefficient with angle of sideslip. M = 5.0; $\alpha = 2.1°$; q ≈ 670 lb/sq ft.

control resulted in a small change in pitch attitude and a large change in angle-of-attack indication. This condition also exists for indicated sideslip angle when the BCS for yaw control is activated.

Angle-of-sideslip measurements.– The characteristics of the spherical sensor for sideslip-angle indications are represented in figure 15 by the variation of the side-force coefficient with sideslip angle for a nominal Mach number of 5.0 at a nominal dynamic pressure of 670 lb/sq ft and an angle of attack of 2.1°. The consistency of the flight data, obtained from several flights, appears to be good. The faired curve of wind-tunnel data is included for comparison. The slopes correlate well; however, a discrepancy of about 0.5° exists in absolute values. This discrepancy may be attributable to the factors mentioned for the angle-of-attack comparison, as well as to possible misalinement of the sensor with the airplane axis and a possible slight asymmetry in the airplane. Probable sensor-housing lip-interference effects are not a problem in sensing angle of sideslip because of the small sideslip excursions of the airplane.

CONCLUDING REMARKS

The spherical flow-direction sensor designed to be used on the X-15 airplane and to advance the state of the art in measuring angle of attack and angle of sideslip in the hypersonic regions of flight up to a Mach number of approximately 7 has fulfilled its objectives and is in operational use. However, upwash effects on the sensor at subsonic speeds caused the indicated values of angle of attack and angle of sideslip to be appreciably higher than the true values, thereby requiring additional pilot attention while flying in this speed range.

The reliability of the sensor has been enhanced by improved inspection techniques to minimize contamination, replacement of vibration-sensitive components by insensitive components, and replacement of quick-disconnect features on plumbing with stainless-steel fittings that comply with military specifications. Improved sensor performance has been realized by replacing the synchro receiver with a passive rotor driven by a servo recorder. A potentially dangerous 12-cycle-oscillation limit-cycle characteristic was alleviated by decreasing the electronic gain and increasing the mechanical gain of the gain-compensation loop.

Although a direct, simultaneous comparison with other flow-direction sensors could not be made because of operational limitations, flight results showed a good consistency in the spherical-sensor data at discrete Mach numbers up to about 6 and at dynamic pressures above 20 lb/sq ft. The spherical-sensor data correlated well with available flight-determined vane-boom data up to a Mach number of approximately 3. A comparison with faired wind-tunnel data showed good correlation in the slope of normal-force coefficient versus angle of attack up through Mach 5.8 and in absolute magnitudes of these parameters up to Mach 3. Above Mach 3, a discrepancy of 1° to 1.5° is evident in angle-of-attack values for comparable flight-sensor and wind-tunnel results.

All factors considered, it is believed that the inherent accuracy of the sensor is better than ±0.5° within the angle-of-attack range of the flight data shown.

At low dynamic pressures, of the order of 40 lb/sq ft and less, it is possible to get erroneous indications of angle of attack at values above approximately 26°, possibly as a result of flow interference from the collar of the sensor.

Degradation in system accuracy becomes appreciable at dynamic pressures below 10 lb/sq ft. At dynamic pressures of the order of 3 lb/sq ft or less, the pitch and yaw reaction jets of the X-15 ballistic control system affect the flow field over the sphere of the sensor, causing erroneous indications.

Flight Research Center,
National Aeronautics and Space Administration,
Edwards, Calif., August 9, 1965.

REFERENCES

1. Richardson, Norman R.; and Pearson, Albin O.: Wind-Tunnel Calibrations of a Combined Pitot-Static Tube, Vane-Type Flow-Direction Transmitter, and Stagnation-Temperature Element at Mach Numbers From 0.60 to 2.87. NASA TN D-122, 1959.

2. Cary, John P.; and Keener, Earl R.: Flight Evaluation of the X-15 Ball-Nose Flow-Direction Sensor as an Air-Data System. NASA TN D-2923, 1965.

3. Anon.: Summary Test Report - N.A.S.A. Flow Direction and Pitot-Pressure Sensor. NORT 59-142, Nortronics, Div. of Northrop Corp., 1959.

4. Anon.: Technical Description and Operating Instructions - N.A.S.A. Flow-Direction and Pitot-Pressure Sensor. NORT 60-46, Nortronics, Div. of Northrop Corp., 1960.

5. Anon.: Revised Basic Aerodynamic Characteristics of the X-15 Research Airplane. Rep. NA-59-1203, (Contract AF33(600) - 31693), North American Aviation, Inc., Aug. 7, 1959.

NASA-Langley, 1965 H-387